SIAM J. APPL. MATH.
Vol. 67, No. 4, pp. 1016–1040

THE FORMATION OF RIVER CHANNELS*

A. C. FOWLER†, NATALIA KOPTEVA‡, AND CHARLES OAKLEY†

Abstract. We consider a deterministic model of landscape evolution through the mechanism of overland flow over an erodible substrate, using the St. Venant equations of hydraulics together with the Exner equation for hillslope erosion. A novelty in the model is the allowance for a nonzero bedload layer thickness, which is necessary to distinguish between transport limited and detachment limited sediment removal. It has long been known that transport limited uniform flow is unstable when the hillslope topography is geomorphologically concave (i.e., the center of curvature is above ground). In this paper, we show how finite amplitude development of the consequent channel flow leads to an evolution equation for its depth h of the form $h_t = h^{3/2} + (h^{3/2})_{YY}$, where Y is the cross-stream space variable. We show that solutions of compact support exist but that, despite appearances, blow up does not occur because of an associated integral constraint, and the channel equation admits a unique and apparently globally stable steady state. The consequences for hillslope evolution models are discussed.

Key words. river networks, mathematical geomorphology, channel formation, nonlinear diffusion

AMS subject classifications. 86A99, 35K55, 35K65

DOI. 10.1137/050629264

1. Introduction.

The formation of river networks is one of a class of morphological problems in which fractal structures are generated by an instability in the medium. Other familiar examples are the lungs, blood capillary beds, and underground limestone cave systems. Two questions immediately present themselves in connection with such structures. The first is whether it is possible to explain quantitatively the basic mechanisms which are involved in causing them to form. The second is the consequent deeper issue of whether it is possible to explain and predict the fractal structures which are observed in nature, given that the model will originate as a deterministic set of differential equations. In this paper, we will be concerned with the first of these questions.

The basic way in which landscape evolves under fluvial erosion is this. Tectonic processes cause uplift of mountain belts, and as the mountains are raised, erosion due to rainfall and runoff causes a gradual lowering of the topography. Other processes, such as glacial erosion and landslides, contribute more dramatically: glaciation at high altitudes, and landslides in regions of higher relief. As is evident from Figure 1, this balance between uplift and erosion is unstable, and the runoff is concentrated into small river channels which drain the catchment.

In attempting to formulate a model to describe this process, we identify two variables of importance; these are the surface elevation s and the water depth h (Figure 2). These will be described by evolution equations representing conservation

*Received by the editors April 15, 2005; accepted for publication (in revised form) December 7, 2006; published electronically May 10, 2007.
http://www.siam.org/journals/siap/67-4/62926.html
†Mathematical Institute, Oxford University, 24-29 St Giles', Oxford OX1 3LB, England (fowler@maths.ox.ac.uk, oakley@maths.ox.ac.uk). The first author was supported by the University of Limerick to maintain his position as Adjunct Professor. The third author was supported by the EPSRC via a postgraduate studentship.
‡Department of Mathematics and Statistics, University of Limerick, Limerick, Republic of Ireland (natalia.kopteva@ul.ie).

FIG. 1. *Hillslope topography. Photograph courtesy of Gary Parker.*

of sediment and water, respectively.

Smith and Bretherton (1972) presented such a model and found that while there is a uniform steady state solution, it is unstable to the formation of channel-like features. In particular, they associated instability with concavity of the hillslope, i.e., $s_{xx} > 0$, where x is the downslope direction of flow.

The particular way in which this instability is manifested is curious. The physical mechanism is plain enough, that increasing depth causes increased water flow, which in turn causes increased erosion and thus channel deepening. In their linear stability analysis, Smith and Bretherton found that the mathematical cause of instability was an effective lateral diffusion coefficient for hillslope which was negative. This naturally produces instability, but the resulting growth rate is unbounded at short wavelength, and their model is consequently ill-posed. Unsurprisingly, properly resolved numerical solutions of the Smith–Bretherton model are not available.

Another consequence of this ill-posedness is a suspicious absence of wavelength selection. Loewenherz (1991) addressed this issue by carrying out a formal linear stability analysis using normal modes (something Smith and Bretherton did not do), and she extended this to convex/concave slopes using the asymptotic technique of WKB theory (Carrier, Krook, and Pearson (1966)) at high wave number k. She also considered the problem of regularization as $k \to \infty$, by introduction of a (fairly arbitrary) modification to the sediment transport law.

Later (Loewenherz-Lawrence (1994)), she treated the whole problem again, but now starting from the hydrodynamic theory, which is also the starting point for the model we present below. In this way, she was able to identify the cause of the ill-posedness of the Smith–Bretherton theory, which lies in the assumption of equal water and land surface slopes. The small mismatch between these two allows regularization at high wave number, and therefore also wavelength selection.

A different approach to the issue of wavelength selection was taken by Izumi and Parker (1995, 2000), who used a St. Venant overland flow model together with a finite

threshold stress for the onset of erosion to show that there is a preferred wavelength for instability. Their estimate in the earlier paper was 33 m, comparable to observed headwater spacings of order 100 m. A formal stability analysis in the second paper (of a slightly different problem) yielded plausibly similar values.

The next logical steps in the development of this theory are a nonlinear theory for finite depth channel development, and full numerical solution of the governing equations. Progress in the first of these aims was made by Kramer and Marder (1992), who developed a nonlinear evolution equation for channel depth by seeking particular solutions of their hillslope model, which was similar, but by no means identical to, the Smith–Bretherton model. The main difference between their result and that of the present paper is that their model is partially empirical, and the derivation of the channel model is not placed in the context of a formal asymptotic approximation to the full model. This leads to important differences in the way the channel evolution equation is posed.

Kramer and Marder also sought to implement a direct numerical simulation, but here, in common with other authors, they were stymied. The apparent reason for this is that the governing partial differential equations are very stiff in both space and time. Water flow in channels occurs on much shorter space and time scales than hillslope evolution, and such numerical computational studies as there have been have not been able to overcome this difficulty.

In response to this, they adopted a cellular lattice model, with physically motivated rules at the lattice points determining the evolution of water depth and land surface elevation. Such cellular models do produce networks but evidently lack a theoretically based predictive capacity. To a large extent, they provide the computational model of choice for other researchers also (e.g., Howard (1994), Tucker and Slingerland (1994)).

A variant on this was the model developed by Willgoose, Bras, and Rodríguez-Iturbe (1991), which combined physically based erosion and water flow equations with an artificial equation for an indicator function Y. Essentially, Y would switch from $Y = 0$ (hillslope) to $Y = 1$ (channel) when water flow increased beyond a critical threshold. In this way, Willgoose et al. could simulate network formation but again without a physically based predictive criterion.

In a sequence of papers, Smith and his coworkers have developed a semianalytic theory of hillslope and channel evolution. Their work is actually orthogonal to the present paper but will be discussed in some detail here because of the apparent parallelism with our work. Smith, Birnir, and Merchant (1997a) consider a simplified version of the Smith–Bretherton model, and use it to suggest that large time solutions have separable form, which they are able to characterize in terms of a variational principle. Smith, Birnir, and Merchant (1997b) elaborate this description by suggesting that an initially smooth hillslope develops channels on a small scale through the Smith–Bretherton instability; the channels saturate via nonlinearity and then evolve into the long time separable solutions described earlier. These results are obtained numerically. In order to obtain numerical results for the ill-posed Smith–Bretherton model, Smith, Birnir, and Merchant (1997b) used a coarse grid on a small plot (100 m by 100 m with grid spacing 1 m), together with enough numerical diffusion to stabilize the results. Smith, Merchant, and Birnir (2000) develop a theory for the time evolution of the grade line of both alluvial and bedrock channels; the former is modelled by a nonlinear diffusion equation, and the latter is modelled by a nonlinear first-order wave equation. Both theories ignore hillslope evolution and make heuristic assumptions in order to derive the models. Birnir, Smith, and Merchant (2001) develop the

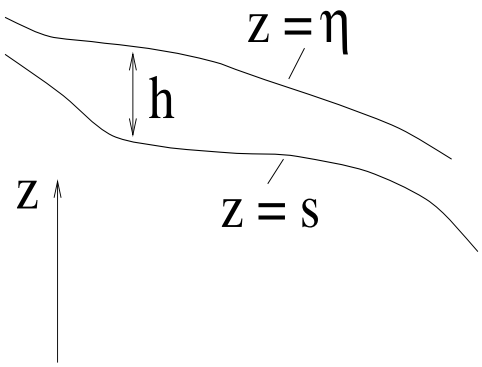

FIG. 2. *Geometry of overland flow.*

ideas originated in the earlier papers by Smith, Birnir, and Merchant (1997a, 1997b). They paint a fairly compelling picture of landscape evolution, which hinges on the twin hypotheses that small scale shock formation in overland flow acts as a seed for white noise to drive the slower hillslope evolution towards a self-similar (separable in time) mature landscape. Crucial to this notion is the assumption that the numerical results are sufficiently detailed to support it. The numerical procedures are improved over those of Smith, Birnir, and Merchant (1997b), but apparently retain the small plot and coarse grid of the earlier calculations, and are therefore open to the same objection, that the coarse grid in particular allows only mildly unstable results by suppressing the high wave number instabilities. The paper by Welsh, Birnir, and Bertozzi (2006) is similar to that of Smith, Merchant, and Birnir (2000), insofar as it uses the Smith–Bretherton model to assess the evolution of the long profile of a river channel. To do this, it assumes a purely one-dimensional model, so that the channel evolves in isolation from the surrounding hillslope.

Our purpose in this paper is to show that a hydrodynamic model similar to those of Loewenherz-Lawrence (1994) and Tucker and Slingerland (1994) leads formally to the derivation of an evolution equation for channel depth (which resembles that of Kramer and Marder). The solution properties of this equation are studied, and it is shown that, despite a similarity of the channel equation to partial differential equations having blow-up properties, there is a unique steady state solution which is stable. This solution may provide an ingredient for future direct numerical simulations of hillslope evolution.

2. A model for sediment and water transport. The geometric situation we consider is portrayed in Figure 2. The vertical coordinate is z, while x and y are horizontal coordinates. The simplest situation is where overland flow occurs down a plane slope, and in this case we take x in the downstream direction and y across stream. The land surface is $z = s(x, y, t)$, the water surface is $z = \eta(x, y, t)$, and the water depth is h, and thus $h = \eta - s$. This relationship is not exact, because the sedimentary surface is further subdivided into a mobile part and a stationary part. A precise statement is given below in (2.9).

The St. Venant equations of hydraulic flow can be written in the form

$$\begin{aligned} &h_t + \boldsymbol{\nabla}.(h\mathbf{u}) = r, \\ &\mathbf{u}_t + (\mathbf{u}.\boldsymbol{\nabla})\mathbf{u} = -g\boldsymbol{\nabla}\eta - \frac{f|\mathbf{u}|\mathbf{u}}{h}. \end{aligned} \tag{2.1}$$

These represent conservation of water mass and momentum and can be derived from the vertically integrated point forms of the equations. r is the source due to rainfall, $\mathbf{u}$ is the mean velocity, and f is a friction factor in a term which represents the bed stress exerted by the flow, assuming this is turbulent. While this is a good parameterization of the bed friction in channelized flow, it is less obviously appropriate for the very thin films which characterize overland flow. We shall comment further on this below, but for the moment we note that consideration of laminar flow at low flow rates would simply have the effect in the model of changing the term $f|\mathbf{u}|$ in $(2.1)_2$ to a constant k, making quantitative but not conceptual difference to the discussion.

Sediment transport. Sediment transport in rivers occurs, for noncohesive sediments with little clay content, when an appropriately dimensionless shear stress (called the Shields stress) delivered by the river exceeds a certain critical value. The turbulent shear stress is taken to be

$$\boldsymbol{\tau} = f\rho_w|\mathbf{u}|\mathbf{u}, \tag{2.2}$$

where ρ_w is water density. If the sediment particles are of diameter D_s (supposed uniform, for simplicity) at the bed, the streamflow exerts a force of approximately $\boldsymbol{\tau}D_s^2$ on it, and it is this force which causes motion. On a slope, there is an additional force due to gravity, approximately $-\Delta\rho g D_s \boldsymbol{\nabla} s$, where $\Delta\rho = \rho_s - \rho_w$ is the density difference between sediment and water, and g is gravitational acceleration. Thus the net effective stress causing motion is actually

$$\boldsymbol{\tau}_e = \boldsymbol{\tau} - \Delta\rho g D_s \boldsymbol{\nabla} s. \tag{2.3}$$

The Shields stress is

$$\mu = \frac{\tau_e}{\Delta\rho g D_s}, \tag{2.4}$$

and particle motion occurs if $\mu \gtrsim \mu_c \approx 0.05$; the critical value depends to some extent on particle size via the particle Reynolds number.

Particle motion occurs in two ways. Larger particles bounce and roll along the bed, and the resultant transport is called bedload transport. Finer particles are lifted up and carried in suspension. In this paper, we will suppose that only bedload transport is relevant. This assumption is made partly for convenience, partly because it corresponds to the choice of Smith and Bretherton (1972), and partly because it may be an unnecessary elaboration to consider suspended load instead or as well.

Various empirical formulae for bedload transport q_b have been proposed. A popular one is that due to Meyer-Peter and Müller (1948), which takes the form

$$q_b = \left(\frac{\rho_s K}{\rho_w^{1/2}\Delta\rho\, g}\right)(\tau_e - \tau_c)_+^{3/2}, \tag{2.5}$$

where Meyer-Peter and Müller chose values of $K = 8$ and $\mu_c = 0.047$, and the critical stress τ_c is defined by

$$\tau_c = \mu_c \Delta\rho g D_s. \tag{2.6}$$

The units of q_b are kg m^{-1} s^{-1}, i.e., mass per unit stream width per unit time.

It is commonly the case that bedload transport is conceived to occur in a layer of zero thickness, if this is considered at all. Although the moving bedload layer

thickness may indeed be small, it is essential to include it in the model (as did Tucker and Slingerland (1994)), because otherwise a relationship such as (2.5) implies that transport occurs even if the substrate is inerodible bedrock. In fact, we must modify (2.5) so that the bedload transport is zero if the bedload layer thickness is equal to zero.

To be specific, we now suppose that $z = s$ describes the interface between stationary bed and moving bedload, and we suppose that the moving bedload layer has thickness a. If the (constant) porosity of the bed (both mobile and immobile) is ϕ and the bedload transport is $\mathbf{q}_b$, then conservation of mobile sediment implies that

$$\rho_s(1-\phi)a_t + \boldsymbol{\nabla}.\mathbf{q}_b = \rho_s(1-\phi)v_A, \tag{2.7}$$

where v_A is the abrasion or entrainment rate of the immobile bed, measured as a velocity.

The Exner equation which describes land surface evolution can now be written in the form

$$\rho_s(1-\phi)s_t = -\rho_s(1-\phi)v_A \ + \ \rho_s(1-\phi)U, \tag{2.8}$$

where U is the velocity of tectonic uplift, or more generally, baselevel fall. The geometric relation between the various depths is seen to be

$$\eta = s + a + h. \tag{2.9}$$

Equations (2.1), (2.7), (2.8), and (2.9) provide five equations for the five variables η, s, a, h, and $\mathbf{u}$; the abrasion rate v_A and bedload transport $\mathbf{q}_b$ need to be prescribed in constitutive relations.

Abrasion and transport rates. It is a fact of observation that the thickness a of the moving bedload layer in a stream is commonly quite small, perhaps only one or two grain thicknesses (Slingerland, Harbaugh, and Furlong (1994, pp. 80–81)). If the stream flow is very rapid, we might expect the consequently rapidly moving grains to mobilize the grains below them. These considerations suggest that the abrasion rate v_A should be a (nonnegative) decreasing function of a which tends to zero at large a and that it should depend on stream flow. With little to guide us, we make the simplest assumption that $v_A = 0$ for a larger than some constant threshold a_0, although it is not difficult to modify this assumption. When $a \geq a_0$, we have conditions of transport limitation, and when $a < a_0$, we have detachment limitation.

We define a bedload velocity (when $a = a_0$)

$$v_b = \frac{q_b}{\rho_s(1-\phi)a_0}, \tag{2.10}$$

and v_b is a function of τ_e. For example, the Meyer-Peter–Müller law (2.5) gives

$$v_b = \left(\frac{K}{\rho_w^{1/2}\Delta\rho\, g(1-\phi)a_0}\right)(\tau_e - \tau_c)_+^{3/2}. \tag{2.11}$$

The constitutive assumptions we will then make for transport and abrasion rates are

$$\begin{aligned} \mathbf{q}_b &= \rho_s(1-\phi)a v_b\,(\tau_e)\,\mathbf{N}, \\ v_A &= k v_b\,(\tau_e)\left[1 - \frac{a}{a_0}\right]_+; \end{aligned} \tag{2.12}$$

the dimensionless constant k would be expected to be extremely small. The direction of bedload transport is given by the unit vector

$$\mathbf{N} = \frac{\boldsymbol{\tau}_e}{\tau_e}. \tag{2.13}$$

Equations (2.7) and (2.8), for mobile and immobile bed surface, respectively, can now be written in the form

$$\begin{aligned} a_t + \boldsymbol{\nabla}.[av_b\mathbf{N}] &= v_A, \\ s_t &= -v_A + U. \end{aligned} \tag{2.14}$$

Nondimensionalization. We choose scales for the variables h, $\mathbf{u}$, η, s, a, τ_e, as well as $\mathbf{x}$ and t, by balancing suitable terms in the governing equations. Suppose that d is a suitable hillslope height scale and l is a suitable horizontal length scale; then we choose

$$\begin{aligned} &r \sim r_D, \quad U \sim U_D, \quad v_b \sim v_D, \quad v_A \sim U_D, \\ &\eta,\ s \sim d, \quad \mathbf{x} \sim l, \quad t \sim [t] = \frac{d}{U_D}, \quad \tau_e \sim [\tau] = f\rho_w\,[u]^2, \\ &\mathbf{u} \sim [u] = \left(\frac{gr_D d}{f}\right)^{1/3}, \quad a \sim a_0, \quad h \sim [h] = l\left(\frac{fr_D^2}{gd}\right)^{1/3}, \end{aligned} \tag{2.15}$$

where square-bracketed terms indicate scales, r_D and U_D are typical precipitation and uplift rates, and for the Meyer-Peter–Müller law (2.11) we would define

$$v_D = \left(\frac{K[\tau]^{3/2}}{\rho_w^{1/2}\Delta\rho\, g(1-\phi)a_0}\right). \tag{2.16}$$

The choice of l is determined by the implied tectonic setting. The simplest conceptual idea is the continuing uplift of an island (or mountain belt), with sea level fixed at prescribed boundaries, and this determines a natural length scale l, the scale of the island. Similarly, crustal folding determines l via the folding wave length. The other length scale d is fixed by the balance of uplift rate with hillslope denudation, which requires (since $v_A \sim U_D$ and also $v_A \sim kv_D$) that

$$U_D = kv_D. \tag{2.17}$$

This determines d through the dependence of v_D on $[\tau]$ and thus $[u]$. For example, if we take v_D to be given by (2.16), then we find

$$d = \left(\frac{\Delta\rho(1-\phi)}{Kf^{1/2}\rho_w}\right)\frac{a_0U_D}{kr_D}. \tag{2.18}$$

The first bracketed term is a constant of $O(1)$, and so we see that the depth scale $d \sim \frac{a_0U_D}{kr_D}$; high mountains are (in this theory) a consequence of high uplift rate and low rainfall, which makes intuitive sense. In addition, the thickness (a_0) and abrasiveness (k) of the bedload layer are crucial in determining d. In practice, we will actually use observed estimates for d to infer suitable values for k.

Using the scaled variables in the model equations (2.1), (2.9), (2.7), and (2.8), we obtain the dimensionless set (where now all the variables refer to the dimensionless

quantities)

$$\begin{aligned} \delta\varepsilon h_t + \boldsymbol{\nabla}.(h\mathbf{u}) &= r, \\ \delta F^2[\,\delta\varepsilon\mathbf{u}_t + (\mathbf{u}.\boldsymbol{\nabla})\mathbf{u}] &= -\boldsymbol{\nabla}\eta - \frac{|\mathbf{u}|\mathbf{u}}{h}, \\ \eta &= s + \delta h + \delta\nu a, \\ \delta\nu\alpha a_t + \boldsymbol{\nabla}.[aV\mathbf{N}] &= \alpha A, \\ s_t &= -A + U, \\ \boldsymbol{\tau}_e &= |\mathbf{u}|\mathbf{u} - \beta\boldsymbol{\nabla}s, \end{aligned} \tag{2.19}$$

where the dimensionless bedload velocity V and abrasion rate A are given, from (2.11) and $(2.12)_2$, by

$$V = [\tau_e - \tau_c^*]_+^{3/2}, \quad A = [1-a]_+ V, \tag{2.20}$$

and the parameters are given by

$$F = \frac{[u]}{(g[h])^{1/2}}, \quad \varepsilon = \frac{U_D}{r_D}, \quad \delta = \frac{[h]}{d},$$

$$\nu = \frac{a_0}{[h]}, \quad \alpha = \frac{kl}{a_0} = \frac{lU_D}{a_0 v_D}, \quad \beta = \frac{\Delta\rho\, D_s}{\rho_w [h]}. \tag{2.21}$$

The dimensionless critical stress can be written in the form

$$\tau_c^* = \frac{\Delta\rho}{\rho_w}\frac{D_s}{[h]}\frac{\mu_c l}{d}, \tag{2.22}$$

which sets out simply how the size of this parameter is determined by the hillslope aspect ratio and by the ratio of water film depth to grain size. μ_c is the dimensionless critical Shields stress, defined in (2.6), and differs from τ_c^* because of the way in which we have nondimensionalized the bed stress.

Parameter estimation. Typical values of precipitation and uplift are $r_D \sim 1$ m y^{-1}, $U_D \sim 10^{-3}$ m y^{-1} (1 km per million years). There is some flexibility in the choice of length scales l and d. Let us suppose that $d \sim 10^3$ m, $l \sim 10^5$ m (i.e., one kilometer uplift over a distance of 100 km) and that $f \sim 0.1$ and $g \sim 10$ m s^{-2}. From these, we find

$$[u] \sim 0.15 \text{ m s}^{-1}, \quad [h] \sim 2.2 \text{ cm}. \tag{2.23}$$

Let us additionally suppose that $a_0 \sim D_s \sim 1$ mm, $\Delta\rho/\rho_w = 2$. It then follows that

$$\begin{gathered} F^2 \sim 0.1, \quad \varepsilon \sim 10^{-3}, \quad \delta \sim 10^{-5}, \\ \alpha \sim 0.1, \quad \beta \sim 0.1, \quad \nu \sim 0.05, \quad \tau_c^* \sim 0.5. \end{gathered} \tag{2.24}$$

It should be emphasized that there is some flexibility in the values of these parameters, but they are all less than one, and in particular ε and δ are very small. It is then legitimate to neglect all the terms proportional to δ in the model. We shall find later that this is a singular approximation, and in order to regularize it we will need at least some of the δ terms to be retained. Apparently, the largest such term is δh in the definition of η, and we therefore choose to retain this term only. It will be easy

to check a posteriori that the neglected terms indeed remain small when the δh term becomes significant.

With the neglect of the terms in δ excluding this excepted term, we derive the reduced model

$$\begin{aligned} \boldsymbol{\nabla}.(h\mathbf{u}) &= r, \\ \mathbf{0} &= -\boldsymbol{\nabla}\eta - \frac{|\mathbf{u}|\mathbf{u}}{h}, \\ \eta &= s + \delta h, \\ \boldsymbol{\nabla}.[aV\mathbf{N}] &= \alpha A, \\ s_t &= -A + U, \\ \boldsymbol{\tau}_e &= |\mathbf{u}|\mathbf{u} - \beta\boldsymbol{\nabla}s. \end{aligned} \tag{2.25}$$

The downslope normal $\mathbf{N}$ is still defined by (2.13).

In order to prescribe boundary conditions for (2.25), consider the uplift of an island continent D with a boundary ∂D; the natural conditions to apply are then

$$\eta = 0 \quad \text{and} \quad \frac{\partial \eta}{\partial n} = 0 \quad \text{on} \quad \partial D. \tag{2.26}$$

These represent the idea that the water surface gradient becomes equal to the ocean gradient (zero) at the coastline. Because the equation for η is essentially elliptic (see the first two equations in (2.25)), the extra condition in (2.26) locates the precise position of the shoreline. Because δ is small, the shoreline position ∂D is essentially known. It will be seen that these conditions are sufficient, together with an initial condition for s, to determine the solution.

A comment on bedload transport. For a given water flow and depth, and thus constant V, the solution for a is $a = 1-\exp(-\alpha x)$, where x is the direction of flow, and assuming that $a = 0$ initially. Thus when $\alpha \gg 1$, we have conditions of transport limitation, and when $\alpha \ll 1$, the transport is detachment limited. The parameter α is the ratio of two small numbers (see (2.21)): k, the ratio of abrasion velocity to bedload velocity (see (2.12)), and a_0/l, the ratio of bedload layer thickness to regional length scale. Its size therefore depends critically on our assumptions about abrasion and bedload. It is plausible that $\alpha \ll 1$ is the more appropriate condition in a regional context over long geological time scales, as suggested by Howard (1994), but this will depend on the friability of the underlying rock. In the laboratory, however, α can be much larger than one because the abrasion coefficient k is likely to be close to one for noncohesive sediments. Simply, noncohesive sediment is eroded and removed rapidly in the field, and over longer time scales, detachment limitation is more appropriate.

A comment on time scales. Although the model and the associated parameter values derived above are consistent with observation, it is unrealistic in the sense that, for example, rainfall is not continuous, and there is no continual overland flow. Rather, erosion actually occurs during severe storms and is virtually absent between them. In a sense, time is not a continuous variable, and it may be more appropriate to switch on the erosional part of the model only during storms. The consequence of this would be a much higher value of r_D, with consequent changes in the parameter values. Despite this, it is still robustly the case that $\delta \ll 1$, and so it seems that the model may be suitable in any case; this, at least, is our assumption.

3. Linear stability. In this section, we review the stability results of Smith and Bretherton (1972) and Loewenherz-Lawrence (1994). We define the downstream flow direction by

$$\mathbf{n} = -\frac{\boldsymbol{\nabla}\eta}{|\boldsymbol{\nabla}\eta|}, \tag{3.1}$$

the stream slope as

$$S = |\boldsymbol{\nabla}\eta|, \tag{3.2}$$

and the water flux as

$$q = h|\mathbf{u}|. \tag{3.3}$$

From (2.25), we then have

$$\boldsymbol{\nabla}.[q\mathbf{n}] = r,$$

$$q = h^{3/2}S^{1/2}, \tag{3.4}$$

and the effective stress is

$$\boldsymbol{\tau}_e = -(h+\beta)\boldsymbol{\nabla}\eta + \delta\beta\boldsymbol{\nabla}h. \tag{3.5}$$

In order to relate our model to those of previous authors, we begin by making corresponding assumptions about bed abrasion and transport. In essence, the prescription of the abrasion rate A in (2.25) is replaced by an assumption that the bedload layer thickness a is constant, $a = 1$. In this case, A is determined by the model, and the bed evolution equation is

$$s_t = U - \frac{1}{\alpha}\boldsymbol{\nabla}.[V\mathbf{N}]. \tag{3.6}$$

This form of the equation is in fact what is obtained in transport limiting conditions when A is prescribed and $\alpha \gg 1$. If A is not prescribed, then the constant k is undefined, so that (2.17) cannot be used to define d. Instead, we define d by choosing $\alpha = 1$, which leads (via (2.21)) to

$$d = \left(\frac{\Delta\rho(1-\phi)}{Kf^{1/2}\rho_w}\right)\frac{lU_D}{r_D}, \tag{3.7}$$

which can be compared with (2.18). For the time being, we assume this to be the case.

Now let us consider the evolution of (one side of) a unidirectional hillslope as shown in Figure 3; that is, we suppose the equations (2.25) are to be solved in the domain $0 < x < 1$, $-L < y < L$, where x is the downslope direction. Suitable boundary conditions are for there to be zero normal flux of sediment and water at the ridge and the two sides, and $\eta = 0$ at $x = 1$. (The extra condition $\eta_x = 0$ at the shoreline is used to locate its precise position near $x = 1$.)

If we take r and U to be constant (more generally, they could be functions of x), then there is a steady state solution for hillslope and water flux; we denote the

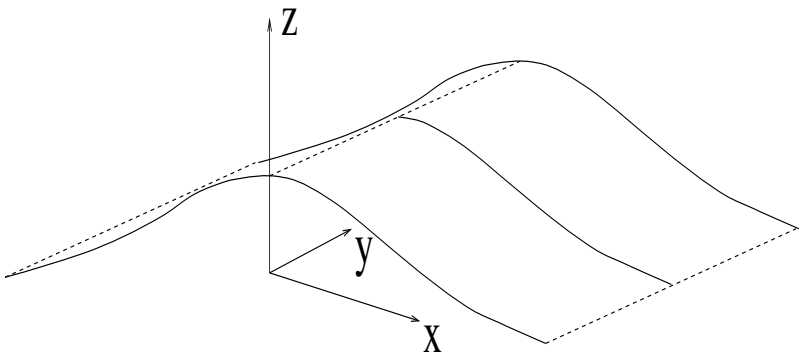

FIG. 3. *One-dimensional hillslope geometry.*

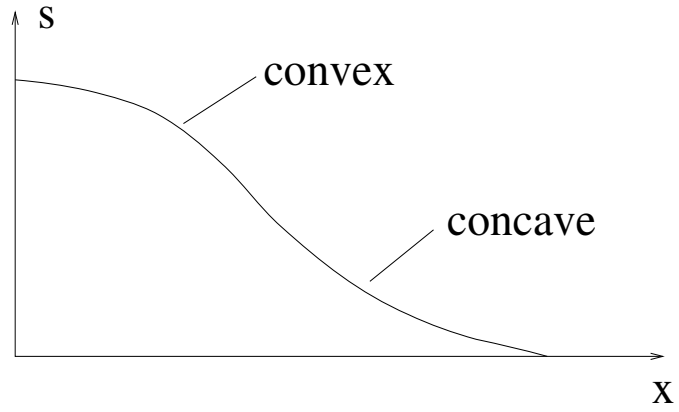

FIG. 4. *Convexity and concavity.*

steady hillslope profile by $\eta = \eta_0(x)$. Smith and Bretherton (1972) showed that for this steady state

$$x\frac{\partial V}{\partial S}S' = V - q\frac{\partial V}{\partial q}, \tag{3.8}$$

where the bedload transport function V is taken to be a function of q and S. (This can be done only if the term in δ is ignored.) Somewhat confusingly, geomorphologists term a slope with $S' < 0$ concave (see Figure 4) or, better, concave upwards, and we shall follow this practice.

As we expect, $\partial V/\partial S > 0$, and this implies that a slope is geomorphologically concave if $\partial V/\partial q > V/q$, and in particular for mathematically convex functions V. We shall find that geomorphologically concave slopes are unstable to channel formation. To leading order in δ, (3.4) and (3.5) imply

$$\tau_e = (qS)^{2/3} + \beta S, \tag{3.9}$$

and so the dimensionless Meyer-Peter–Müller relationship in (2.20), for example, can be written in the form

$$V = [(qS)^{2/3} + \beta S - \tau_c^*]_+^{3/2}. \tag{3.10}$$

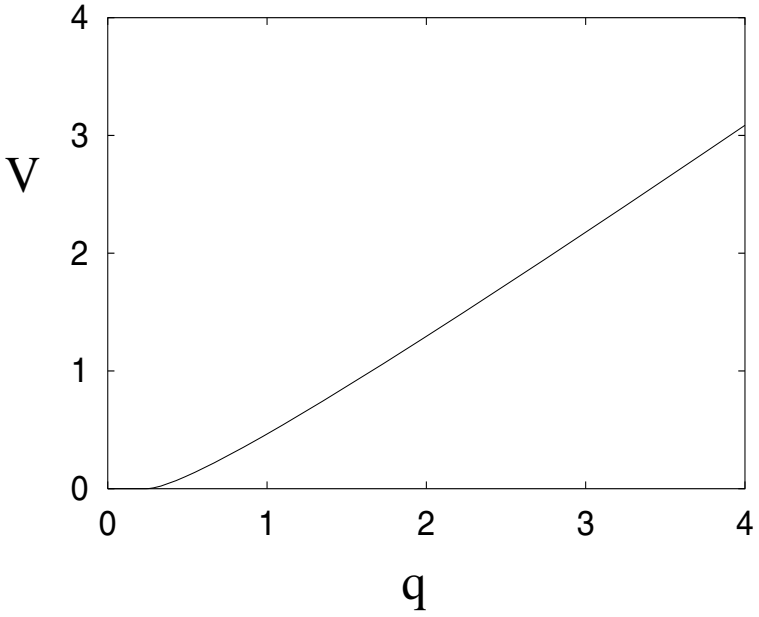

FIG. 5. $V(q,S)$ *given by* (3.10) *for* $\beta = 0.1$, $\tau_c^* = 0.5$.

Figure 5 shows that this relation typically produces a (weakly) mathematically convex function and hence a weakly concave upward hillslope.

Our aim is study perturbations to the steady state $\eta = \eta_0(x)$. Even if the water depth perturbations are large, we can still linearize the geometry of the directions $\mathbf{n}$ and $\mathbf{N}$ by expanding in terms of δ. We do this first. In the one-dimensional steady state, $\mathbf{N} = \mathbf{n} = \mathbf{i}$. We put

$$\eta = \eta_0 + \tilde{\eta}, \tag{3.11}$$

and suppose that $\tilde{\eta}$ is small. We then find

$$\begin{aligned} \boldsymbol{\nabla}\eta &= \eta_0'\mathbf{i} + \boldsymbol{\nabla}\tilde{\eta}, \\ |\boldsymbol{\nabla}\eta| = S &= S_0 - \tilde{\eta}_x + \cdots, \end{aligned} \tag{3.12}$$

where the steady state slope is

$$S_0 = |\eta_0'|. \tag{3.13}$$

Thus

$$\begin{aligned} \mathbf{n} &= \mathbf{i} - \frac{\tilde{\eta}_y}{S_0}\mathbf{j} + \cdots, \\ q &= h^{3/2}S^{1/2}, \end{aligned} \tag{3.14}$$

and in a similar way we find (if also δh is small)

$$\begin{aligned} \tau_e &= (h+\beta)S + \delta\beta h_x + \cdots, \\ \mathbf{N} &= \mathbf{i} - \frac{1}{S_0}\left\{\tilde{\eta}_y - \frac{\delta\beta}{h+\beta}h_y\right\}\mathbf{j} + \cdots. \end{aligned} \tag{3.15}$$

Adopting for the moment only these approximations (that is, we linearize the geometry only), we derive from (3.4) and (3.6) the following approximate model:

$$\frac{\partial q}{\partial x} - \frac{\partial}{\partial y}\left[\frac{q}{S_0}\frac{\partial \tilde{\eta}}{\partial y}\right] = r,$$

$$\frac{\partial \tilde{\eta}}{\partial t} - \delta\frac{\partial h}{\partial t} = U - \frac{\partial V}{\partial x} + \frac{\partial}{\partial y}\left[\frac{V}{S_0}\left\{\frac{\partial \tilde{\eta}}{\partial y} - \frac{\beta\delta}{h+\beta}\frac{\partial h}{\partial y}\right\}\right], \tag{3.16}$$

with q and τ_e defined in (3.14) and (3.15). Notice that this model is still nonlinear.

If the steady solution in which $q_0 = rx$ and $V_0 = Ux$ of this pair of equations is linearized, then what we find is the following. If we put $\delta = 0$ (and thus $V = V(q, S)$), instability occurs if $\partial V/\partial q > V/q$ at any point, as stated above, and the growth rate is unbounded ($\propto k^2$) as the lateral wave number k of modes $\propto e^{iky}$ increases. This implies ill-posedness of the model with $\delta = 0$. If $\delta > 0$ but is small, then the system is stabilized at high wave number. More detailed consideration of the linear eigenvalue problem suggests that instability occurs for k in the range $O\left(\frac{1}{\delta^{1/2}}\right) < k < O\left(\frac{1}{\delta}\right)$, and that maximal growth occurs for $k = O\left(\frac{1}{\delta^{3/4}}\right)$. Oscillations in the x direction are stabilizing.

In dimensional terms, the range of unstable wavelengths l_u is thus in the range

$$\frac{[h]l}{d} < l_u < \frac{[h]^{1/2}l}{d^{1/2}}, \tag{3.17}$$

and thus it bears no simple relation to any of the three geometric length scales of the problem but involves them all.

Because $\delta \ll 1$, i.e., $[h] \ll l$, the result in (3.17) suggests that a nonlinear theory for channel formation can be based on the fact that the lateral length scale for growing perturbations is much smaller than the downstream length scale; in other words, we now turn to a direct asymptotic solution of (3.16) when h is large.

4. An evolution equation for channel formation. The discussion above of linear stability when $\delta \ll 1$ suggests that a distinguished lateral length scale of order $\lesssim \delta^{1/2}$ may serve to delineate the unstable growth of rills. Let us now focus on this growth by defining

$$y = \delta^{1/2}Y, \quad \tilde{\eta} = \delta Z, \quad t = \delta\tilde{t}; \tag{4.1}$$

the rescaling of $\tilde{\eta}$ and t is motivated by the linear stability result of Loewenherz-Lawrence (1994), which suggests that when $y \sim 1/k \ll 1$, then $\tilde{\eta} \sim \tilde{q}/k^2$, or more generally $\tilde{\eta} \sim h^{3/2}/k^2$, and $t \sim 1/k^2$. For $k \sim 1/\delta^{1/2}$ and $h \sim O(1)$, we obtain (4.1). Note that if the original time scale $\sim d/U_D$ was 10^6 years, then this new time scale is $[h]/U_D$ (film thickness divided by uplift or erosion rate), of order 10 years.

The equations (3.16) retain their validity based on geometric linearity, and take the form

$$\frac{\partial q}{\partial x} - \frac{\partial}{\partial Y}\left[\frac{q}{S}\frac{\partial Z}{\partial Y}\right] = r,$$

$$\frac{\partial Z}{\partial \tilde{t}} - \frac{\partial h}{\partial \tilde{t}} = U - \frac{\partial V}{\partial x} + \frac{\partial}{\partial Y}\left[\frac{V}{S}\left\{\frac{\partial Z}{\partial Y} - \frac{\beta}{h+\beta}\frac{\partial h}{\partial Y}\right\}\right], \tag{4.2}$$

in which $S(x)$ is the steady slope (i.e., such that $Z = 0$ is a solution of (4.2)), and the water flux q and effective driving stress for sediment transport τ_e are given by

$$\tau_e \approx (h+\beta)S, \quad q = h^{3/2}S^{1/2}. \tag{4.3}$$

To be specific, we pose these equations on a rectangular domain $-L < y < L$ (thus $-L/\delta^{1/2} < Y < L/\delta^{1/2}$) and $0 < x < 1$. In terms of x and y, the no flux and shoreline boundary conditions require

$$\begin{aligned} \frac{\partial h}{\partial y} = \frac{\partial Z}{\partial y} = 0 \quad &\text{on} \quad y = \pm L, \\ q = V = 0 \quad &\text{on} \quad x = 0, \\ Z = 0 \quad &\text{on} \quad x = 1. \end{aligned} \tag{4.4}$$

These equations enclose the linear instability of the steady state (on a lateral space scale $Y = O(1)$, and time scale $\tilde{t} = O(1)$); but they are fully nonlinear equations and may provide a vehicle to understand the nonlinear development of the linear rill instability we have found before.

One possibility is that stable finite amplitude solutions (rills) exist for this model, with $h \sim O(1)$. Such rills have depths of order millimeters or centimeters, and do not correspond to larger river channels, which presumably evolve over longer geological time scales, possibly by coarsening and scale evolution.

We make the supposition that larger channels can evolve in this model, and therefore we seek solutions representing such large channels in which the depth $h \gg 1$, and where it is a function of the short length scale $Y \sim O(1)$. Note that a consequence of $(4.2)_1$ is that

$$\int_{-L/\delta^{1/2}}^{L/\delta^{1/2}} q \, dY = 2Lrx/\delta^{1/2}, \tag{4.5}$$

which serves as a constraint on the channel depth. In particular, (4.3) suggests a distinguished limit $h \sim 1/\delta^{1/3}$ when most of the rainfall finds its way into the channel. Thus we rescale the variables as

$$h = \frac{H}{\delta^{1/3}}, \quad q = \frac{Q}{\delta^{1/2}}, \quad V = \frac{F}{\delta^{1/2}}, \quad \tau_e = \frac{T_e}{\delta^{1/3}}, \quad \tilde{t} = \delta^{1/6} T. \tag{4.6}$$

(This assumes that $V \sim \tau_e^{3/2}$ for large τ_e, as is the case for the Meyer-Peter relation in (2.20).) With $\delta \approx 10^{-5}$, then $1/\delta^{1/3} \approx 46$, and the new depth scale is of the order of a meter, sensible for a developed stream. The choice of time scale (corresponding dimensionally to a year) is so that the time derivative of h in $(4.2)_2$ is balanced. On the other hand, we expect the water surface to remain flat, so that we do not seek to rescale Z: as we will see, this is consistent with the model equations.

Introducing (4.6) into (4.2) and (4.3), we obtain

$$\begin{aligned} \frac{\partial Q}{\partial x} - \frac{\partial}{\partial Y}\left[\frac{Q}{S}\frac{\partial Z}{\partial Y}\right] &= \delta^{1/2} r, \\ \delta^{1/2}\frac{\partial Z}{\partial T} - \frac{\partial H}{\partial T} &= \delta^{1/2} U - \frac{\partial F}{\partial x} + \frac{\partial}{\partial Y}\left[\frac{F}{S}\left\{\frac{\partial Z}{\partial Y} - \frac{\beta}{H + \delta^{1/3}\beta}\frac{\partial H}{\partial Y}\right\}\right], \end{aligned} \tag{4.7}$$

$$T_e \approx (H + \delta^{1/3}\beta)S, \quad Q = H^{3/2} S^{1/2}. \tag{4.8}$$

The rescaled sediment transport function F is only $O(1)$ with this rescaling if $F \sim \tau_e^{3/2}$, which is of course precisely true for the Meyer-Peter–Müller law:

$$F = \left[T_e - \delta^{1/3}\tau_c^*\right]_+^{3/2}. \tag{4.9}$$

Any other choice of transport law would require a more contorted rescaling.

We can use (4.8) to write (4.9) in the form

$$F = QS + \tfrac{3}{2}(\delta QS)^{1/3}(\beta S - \tau_c^*) + \cdots . \tag{4.10}$$

Simplification of $(4.7)_2$ now yields

$$-\delta^{1/2}\frac{\partial Z}{\partial T} + \frac{\partial H}{\partial T} = S'S^{1/2}H^{3/2} + S^{1/2}\frac{\partial}{\partial Y}\left[\beta H^{1/2}\frac{\partial H}{\partial Y}\right] + C\frac{\partial^2 Z}{\partial Y^2}, \tag{4.11}$$

with inessential error terms of $O(\delta^{1/3})$. The instability parameter C is given by

$$C = \frac{Q}{S}\left(F_Q - \frac{F}{Q}\right) \approx -\delta^{1/3}(\beta S - \tau_c^*)\left(\frac{H}{S}\right)^{1/2}. \tag{4.12}$$

It is a peculiarity of the Meyer-Peter–Müller law that $C = 0$ to leading order, so that the steady state is approximately neutrally linearly stable (at these large stresses). This is because at leading order F is linear in Q, and the function is neither mathematically convex nor concave

Equation (4.11) reveals the essence of linear instability and its nonlinear development. Linear instability is associated with the negative diffusion coefficient of Z if $C > 0$, i.e.,

$$S < S_c = \frac{\tau_c^*}{\beta} = \frac{\mu_c l}{d}, \tag{4.13}$$

using (2.21) and (2.22). In dimensional terms, this suggests instability if the slope is less than μ_c, which occurs at the shoreline. If the resulting rills are able to grow to significant depth, then the nonlinear evolution of H is described approximately by

$$\frac{\partial H}{\partial T} = S'S^{1/2}H^{3/2} + S^{1/2}\frac{\partial}{\partial Y}\left[\beta H^{1/2}\frac{\partial H}{\partial Y}\right], \tag{4.14}$$

and Z then follows from (4.7) by quadrature. Equation (4.14) is a degenerate nonlinear diffusion equation, about which a good deal is known. The source term is suggestive (if $S' > 0$, i.e., on the (upper) convex portion of the hillslope) of blow up and the possibility that H could reach ∞ at a finite time. The degenerate diffusion coefficient is suggestive of solutions of compact support.

The integral constraint (4.5) can be written in the limiting form (as $\delta \to 0$)

$$\int_{-\infty}^{\infty} H^{3/2}\, dY = \frac{2Lrx}{S^{1/2}}. \tag{4.15}$$

Note that this constraint is independent of (4.14), which is derived from sediment conservation, whereas (4.15) is a condition of water mass flow.

Suitable boundary conditions for (4.14) follow from matching to an outer film flow, where $Y \sim 1/\delta^{1/2}$ and $H \sim \delta^{1/3}$. Consequently, we require

$$H \to 0 \quad \text{as} \quad Y \to \pm\infty. \tag{4.16}$$

The initial condition is that H is initially small (since we suppose it arises from an instability of the steady state $H \sim \delta^{1/3}$), i.e.,

$$H \to 0 \quad \text{as} \quad T \to 0. \tag{4.17}$$

The precise behavior of H for small T is less easy to describe. The reason for this is that we have omitted an intermediate discussion of the nonlinear stability of the uniform steady state. The long time evolution of an arbitrary (infinitesimal) perturbation to the steady state can be described by consideration of a Fourier integral over normal modes of wave number k. The upshot of such a consideration is that the emerging linear solution is a monochromatic oscillation whose wave number is that with maximum growth rate, and this would serve as a suitable initial condition for the resulting nonlinear equations in (4.2). However, to obtain an appropriate initial condition for (4.14), we really need to know how solutions to (4.2) behave. We suppose that the nonlinear equations (4.2) do not (always) have stable bounded solutions for H and that (for example) they may exhibit some kind of blow up. In that case, one might expect to obtain a suitable form for the initial behavior of H by matching to the large amplitude solution of (4.2). This is similar to the procedure adopted by Stewartson and Stuart (1971).

In directly seeking solutions at larger amplitude, we are motivated by the fact that developed river channels do indeed attain depths on the order of a meter, and this is consistent with the scale of the solutions described by (4.14).

5. Solution properties. The problem (4.14) with the integral constraint, boundary, and initial conditions (4.15)–(4.17) can be written in normalized form by defining new variables u, t, η (note this is unrelated to the use of η for the water surface in sections 2 and 3) via

$$H = \left(\frac{6}{\beta}\right)^{1/3} (Lrx)^{2/3} u, \quad T = \left(\frac{\beta}{6}\right)^{1/6} \frac{S^{1/2} S'}{(Lrx)^{1/3}} t, \quad Y = \left(\frac{2\beta}{3S'}\right)^{1/2} \eta, \tag{5.1}$$

whence we find

$$u_t = u^{3/2} + \left(u^{3/2}\right)_{\eta\eta},$$

$$\int_{-\infty}^{\infty} u^{3/2}\, d\eta = 1, \quad u \to 0 \quad \text{as} \quad \eta \to \pm\infty, \quad t \to 0. \tag{5.2}$$

This equation has been much studied by pure mathematicians, and it features prominently in the book by Samarskii et al. (1995), where numerous results concerning blow up and localization (i.e., attainment of compact support) are proved. The results in this book are, however, concerned with smooth solutions, for which blow up is essentially obvious; that is, for solutions of compact support, it is assumed that the derivative of u is zero at the boundary of the support. The derivation of the same equation here from a real physical model is clearly of some interest, but it is clearly incorrect to suppose that solutions will necessarily have zero derivative at the support margin. In general, the derivatives are finite at the margins, and in fact blow up does not occur (which, physically, is an appropriate behavior).

In our investigation of the solutions of (5.2), we are led to assert the following. A solution of the problem exists, and there is a unique steady state which is globally stable and of compact support. Starting from an initial condition of infinite support, the solution attains finite support immediately (i.e., for all $t > 0$). We have not proved these results, but we show why we think they are true in the following subsections.

Steady state and linear stability. We will limit our attention to symmetric solutions, so that u is even, and $u_\eta = 0$ on $\eta = 0$. It is convenient to define

$$v = u^{3/2}, \tag{5.3}$$

and we note that for symmetric solutions, we have

$$\int_0^\infty v\,d\eta = \tfrac{1}{2}. \tag{5.4}$$

It is trivial to see that there is a unique steady state $v_s(\eta)$, given by

$$v = \tfrac{1}{2}\cos\eta, \quad 0 < \eta < \pi/2,$$
$$v = 0, \quad \eta > \pi/2. \tag{5.5}$$

To examine linear stability, we put

$$v = \tfrac{1}{2}\cos\eta + V, \tag{5.6}$$

and linearize the equations, to obtain

$$\frac{2}{3v_s^{1/3}} V_t = V_{\eta\eta} + V, \tag{5.7}$$

subject to

$$\int_0^{\pi/2} V\,d\eta = 0, \quad V_\eta = 0 \quad \text{at} \quad \eta = 0. \tag{5.8}$$

(The condition on v at the margin determines the motion of the margin.) Separable solutions to this of the form $V = W(\eta)e^{\sigma t}$ exist, and W then satisfies a nonstandard eigenvalue problem. It is convenient to define

$$\phi = W + W_\eta|_{\pi/2}\cos\eta; \tag{5.9}$$

it follows that ϕ satisfies the nonstandard eigenvalue problem

$$\phi'' + \phi = \frac{2\sigma}{3v_s^{1/3}}\left[\phi - v_s\int_0^{\pi/2}\phi\,d\eta\right], \tag{5.10}$$

subject to

$$\phi'(0) = \phi'(\pi/2) = 0. \tag{5.11}$$

Consider for a moment the equation

$$\psi'' + \psi = \lambda\psi, \tag{5.12}$$

subject to

$$\psi'(0) = \psi'(\pi/2) = 0. \tag{5.13}$$

This is a standard eigenvalue problem with eigenfunctions $\cos 2n\eta$ and eigenvalues $\lambda = 1 - 4n^2$, $n \in \mathbf{N}$, and direct integration shows that

$$\lambda = \frac{\displaystyle\int_0^{\pi/2}(\psi^2 - \psi'^2)\,d\eta}{\displaystyle\int_0^{\pi/2}\psi^2\,d\eta}. \tag{5.14}$$

The standard variational formulation for Sturm–Liouville problems then implies that the functional $\lambda(\psi)$ defined by (5.14) is maximized by the principal eigenfunction $\cos 2\eta$, for which $\lambda = -3$. It follows from this that for all functions ϕ satisfying (5.10) and (5.11) (and thus not proportional to this eigenfunction), we have

$$\int_0^{\pi/2} (\phi^2 - \phi'^2)\, d\eta < -3 \int_0^{\pi/2} \phi^2\, d\eta. \tag{5.15}$$

Multiplying (5.10) by ϕ and integrating from 0 to $\pi/2$, we thus have

$$\frac{2\sigma}{3}\left[\int_0^{\pi/2} \frac{\phi^2}{v_s^{1/3}}\, d\eta - \int_0^{\pi/2} v_s^{2/3}\phi\, d\eta \int_0^{\pi/2} \phi\, d\eta\right] = \int_0^{\pi/2} (\phi^2 - \phi'^2)\, d\eta < 0. \tag{5.16}$$

We are assuming for convenience in this exposition that σ is real. The problem (5.10) is not self-adjoint, and so σ may be complex. We leave it as an exercise to show that the proof below that $\sigma < 0$ can be straightforwardly generalized to the result $\operatorname{Re}\sigma < 0$.

From the Cauchy–Schwarz inequality, we have

$$\int_0^{\pi/2} v_s^{2/3}\phi\, d\eta \le \left(\int_0^{\pi/2} v_s^{5/3}\, d\eta\right)^{1/2} \left(\int_0^{\pi/2} \frac{\phi^2}{v_s^{1/3}}\, d\eta\right)^{1/2},$$

$$\int_0^{\pi/2} \phi\, d\eta \le \left(\int_0^{\pi/2} v_s^{1/3}\, d\eta\right)^{1/2} \left(\int_0^{\pi/2} \frac{\phi^2}{v_s^{1/3}}\, d\eta\right)^{1/2}, \tag{5.17}$$

and thus

$$\begin{aligned}\int_0^{\pi/2} v_s^{2/3}\phi\, d\eta \int_0^{\pi/2} \phi\, d\eta &\le \left(\int_0^{\pi/2} v_s^{5/3}\, d\eta \int_0^{\pi/2} v_s^{1/3}\, d\eta\right)^{1/2} \int_0^{\pi/2} \frac{\phi^2}{v_s^{1/3}}\, d\eta \\ &< \frac{\pi}{4} \int_0^{\pi/2} \frac{\phi^2}{v_s^{1/3}}\, d\eta, \end{aligned} \tag{5.18}$$

since $v_s \le \frac{1}{2}$. It follows from this and (5.16) that $\sigma < 0$. More generally, we can prove $\operatorname{Re}\sigma < 0$, so that the steady state is linearly stable as far as the discrete spectrum is concerned.

Front motion. The degeneracy of (5.2) suggests that solutions will be of compact support and that the fronts where $u = 0$ will move at finite speed. The fronts correspond to the location of the margins of the channel. Even if the initial support is unbounded, we suggest below that the solution support instantly becomes finite. It is then of interest to know how the front moves.

We write (5.2) in terms of $v = u^{3/2}$, and thus

$$\frac{2}{3v^{1/3}} v_t = v_{\eta\eta} + v, \tag{5.19}$$

and if the front position is $\eta_m(t)$ (thus $v > 0$ for $\eta < \eta_m$), we assume that near the front,

$$v \sim c(\eta_m - \eta)^\nu + d(\eta_m - \eta)^\mu + \cdots, \tag{5.20}$$

where $\mu > \nu > 0$. Substituting this into (5.19) and balancing the leading-order terms, we obtain $\nu = 3$, $\dot\eta_m = \frac{3}{2}(\nu - 1)c^{1/3}$, and thus

$$v \sim c(\eta_m - \eta)^3, \quad \dot\eta_m \sim 3c^{1/3}. \tag{5.21}$$

In terms of u, this implies

$$u \sim \alpha(\eta_m - \eta)^2, \quad \dot\eta_m \sim 3\sqrt{\alpha}, \tag{5.22}$$

and we see that such solutions are possible only for front advance. In particular, they do not describe the evolution of a channel from the initial conditions in (5.2).

Another balance is possible if $\nu = 1$, when the second-order term in (5.20) comes into play. Balancing of terms then implies $\mu = \frac{5}{3}$, and then

$$v \sim c(\eta_m - \eta) + d(\eta_m - \eta)^{5/3} + \cdots, \quad \dot\eta_m \sim \frac{5d}{3c^{2/3}}. \tag{5.23}$$

In terms of u, this yields

$$u \sim \alpha(\eta_m - \eta)^{2/3} + \beta(\eta_m - \eta)^{4/3} + \cdots, \quad \dot\eta_m \sim \frac{5\beta}{2\sqrt{\alpha}}; \tag{5.24}$$

the slope is infinite at the front, and the direction of motion depends on the coefficient of the higher-order corrective term. Fatter fronts advance, and thinner ones retreat.

Small time solution. We have mentioned above that numerical results are consistent with the idea that the solution immediately becomes of finite support. To examine how this occurs, we study the form of the solution for small t.

It is convenient for the analysis (and also for the numerical solution of the problem) to transform the domain to a fixed interval. A smart way to do this is to define the independent variable

$$s = \int_0^\eta v \, d\eta. \tag{5.25}$$

Changing variables from η, t to s, t leads to the pair of equations for v and η (which now becomes a function of s and t):

$$\begin{gathered} v\eta_s = 1, \\ \frac{2}{3v^{1/3}}[v_t - \eta_t v v_s] = v + v[v v_s]_s, \end{gathered} \tag{5.26}$$

subject to the conditions

$$\begin{aligned} \eta \;=\; & v_s = 0 \quad \text{on} \quad s = 0, \\ & v = 0 \quad \text{on} \quad s = \tfrac{1}{2}, \\ & v = v_0(s) \quad \text{at} \quad t = 0. \end{aligned} \tag{5.27}$$

The front position is then found a posteriori from the equation

$$\eta_m(t) = \eta(\tfrac{1}{2}, t). \tag{5.28}$$

If we take $v_0'(\frac{1}{2})$ to be finite, then the initial support is infinite, $\eta_m(0) = \infty$, and the solution has a singularity at $t = 0$, $s = \frac{1}{2}$. In expanding the solution for small

t, we therefore make use of the method of strained coordinates in order to ensure a uniform expansion. This will enable us to determine the initial position of the front η_m. We define new variables T, ζ via

$$t = \varepsilon T, \quad s = \zeta + \varepsilon s_1(\zeta) + \cdots, \tag{5.29}$$

in terms of which the equations become

$$\begin{aligned} v(1 - \varepsilon s_{1\zeta} \dots)\eta_\zeta &= 1, \\ v_T - \varepsilon s_{1T} v_\zeta \dots - (\eta_T - \varepsilon s_{1T}\eta_\zeta \dots)v(1 - \varepsilon s_{1\zeta} \dots)v_\zeta & \\ = \frac{3}{2}\varepsilon v^{4/3}\left[1 + (1 - \varepsilon s_{1\zeta} \dots)\frac{\partial}{\partial \zeta}\{v(1 - \varepsilon s_{1\zeta} \dots)v_\zeta\}\right]. & \end{aligned} \tag{5.30}$$

Now we seek solutions in the form

$$v \sim v_0 + \varepsilon v_1 \dots, \quad \eta \sim \eta_0 + \varepsilon \eta_1 \dots, \tag{5.31}$$

anticipating that the leading-order solution v_0 is given by the initial function $v_0(\zeta)$. The function s_1 is to be chosen in order to ensure that the expansions in (5.31) are uniformly valid.

Equating powers of ε, we find that at $O(1)$,

$$\begin{aligned} v_0\eta_{0\zeta} &= 1, \\ v_{0T} - \eta_{0T}v_0v_{0\zeta} &= 0. \end{aligned} \tag{5.32}$$

We take the solution of this to be

$$v_0 = v_0(s), \quad \eta_0 = \int_0^\zeta \frac{d\zeta'}{v_0(\zeta')}. \tag{5.33}$$

Then at $O(\varepsilon)$, we find (since $\eta_{0T} = 0$)

$$\begin{aligned} v_0\eta_{1\zeta} + \eta_{0\zeta}v_1 &= s_{1\zeta}, \\ v_{1T} - v_0v_{0\zeta}\eta_{1T} &= \tfrac{3}{2}v_0^{4/3}[1 + (v_0v_{0\zeta})_\zeta]. \end{aligned} \tag{5.34}$$

The conditions we require to be satisfied for the functions η_1, v_1, and s_1 are

$$\begin{aligned} \eta_1 = v_{1\zeta} = s_1 = 0 \quad &\text{on} \quad \zeta = 0, \\ s_1 = v_1 = 0 \quad &\text{at} \quad T = 0. \end{aligned} \tag{5.35}$$

The choice of $s_1 = 0$ ensures that $s = 0$ when $\zeta = 0$ and seems feasible because of the term $s_{1\zeta}$ in $(5.34)_1$; it is less obvious that we will be able to choose $s_1 = 0$ at $T = 0$, but if so, then $s = \zeta$ initially, which allows us to prescribe $v_1 = 0$ initially. Note that there is no boundary condition at the front, as its location in terms of ζ is not known: we do not expect to be able to prescribe $s_1 = 0$ at $\zeta = \frac{1}{2}$.

The solution can be found by eliminating v_1 in (5.34), and we find

$$\begin{aligned} \eta_1 &= \frac{s_1}{v_0} - \frac{3TI(\zeta)}{2v_0}, \\ v_1 &= v_0s_{1\zeta} - v_0^2\eta_{1\zeta}, \end{aligned} \tag{5.36}$$

taking into account the boundary and initial conditions. The function $I(\zeta)$ is defined by

$$I(\zeta) = \int_0^\zeta v_0^{1/3}[1 + (v_0 v_{0\zeta})_\zeta]\, d\zeta'. \tag{5.37}$$

We compute $v_{1\zeta}$ at $\zeta = 0$ and find

$$v_{1\zeta}|_{\zeta=0} = s_1|_{\zeta=0} + \tfrac{3}{2} T v_0^{7/3} v_0'''. \tag{5.38}$$

Because of our assumption of a symmetric solution, v_0 is even, and therefore $v_0'''(0) = 0$. It is because of this that we can consistently choose $s_1 = 0$ at $\zeta = 0$.

Finally, we must specify s_1. This is done by examining the behavior of the solution as $\zeta \to \frac{1}{2}$. We define

$$a = -v_0'(\tfrac{1}{2}). \tag{5.39}$$

Then as $\zeta \to \frac{1}{2}$,

$$v_0 \sim aX, \quad \eta_0 \sim -\frac{1}{a} \ln X + O(1), \tag{5.40}$$

where we write $X = \frac{1}{2} - \zeta$. We thus require s_1 to be such that $v_1 \le O(X)$ and $\eta_1 \le O(\ln X)$. Expanding v_1 and η_1 for small X, we find

$$\begin{aligned} \eta_1 &\sim \frac{s_1}{aX} - \frac{3 I_m T}{2aX} + O(1), \\ v_1 &\sim -a s_1 + \frac{3 I_m a T}{2} \ldots, \end{aligned} \tag{5.41}$$

where

$$I_m = I(\tfrac{1}{2}) = \int_0^{1/2} v_0^{1/3}[1 + (v_0 v_{0\zeta})_\zeta]\, d\zeta'. \tag{5.42}$$

In order to suppress the singular terms, a simple choice of s_1 which also satisfies the requested initial and boundary conditions is

$$s_1 = \tfrac{3}{2} I_m T (1 - 2X). \tag{5.43}$$

Of principal interest is the margin position, which is given implicitly by the pair of equations

$$\begin{aligned} \eta_m &= \eta_0(\zeta) + \varepsilon \eta_1(\zeta, T) + \cdots, \\ \tfrac{1}{2} &= \zeta + \varepsilon s_1(\zeta, T) + \cdots. \end{aligned} \tag{5.44}$$

Using the definitions of η_1 and s_1 and expanding for small ε, we find that the margin position is given in terms of t by the expression

$$\eta_m \approx \frac{1}{a} \ln\left\{\frac{1}{3 I_m t}\right\} + \int_0^{1/2} \left[\frac{1}{v_0(\zeta)} - \frac{1}{a(\frac{1}{2} - \zeta)}\right] d\zeta + O(t). \tag{5.45}$$

This result suggests (but does not prove) that the solution is of compact support for all $t > 0$. The asymptotic form of the front position is consistent with a numerical solution of the problem, as we now describe.

Numerical solution. To solve the system (5.26) and (5.27) numerically, we discretize the equations on uniform meshes. To avoid a sparse mesh in the neighborhood of the endpoint $\eta = \eta_m$, which would occur because of the slow change of s there, we reformulate our problem once again by defining a new positive space variable ξ as

$$(1 - \xi) = \sqrt{1 - 2s}. \tag{5.46}$$

The model can then be written in the form

$$\begin{aligned}
u_t &= \eta_t w u_\xi + w(w v_\xi)_\xi + v \quad \text{for } \xi \in (0,1), \quad t > 0,\\
v &= u^{3/2}, \qquad w = \frac{v}{1-\xi},\\
u_\xi(0,t) &= 0, \qquad u(1,t) = 0,\\
v(\xi,0) &= v_0[s(\xi)],\\
\eta_\xi &= \frac{1-\xi}{v} \quad \text{for } \xi \in (0,1], \quad \eta(0,t) = 0, \quad t \geq 0,
\end{aligned} \tag{5.47}$$

where now $u = u(\xi,t)$, $v = v(\xi,t)$, and $\eta = \eta(\xi,t)$. Furthermore, we now have

$$\eta_m(t) = \eta(1,t).$$

We discretize in time using the first-order explicit Euler method and in space using second-order finite differences on uniform meshes. Hence the time step τ is chosen much smaller than the space mesh size N^{-1}.

Approximations of η are computed at each time level by numerical integration of $(5.47)_5$ and thus will be $O(N^{-2})$-accurate. If we evaluated η_t in $(5.47)_1$ using these computed approximations of η, we would introduce huge errors of order N^{-2}/τ in the discretization of $(5.47)_1$ and fail to get accurate computed solutions. More accurate approximations of η_t are obtained by differentiating $(5.47)_5$ with respect to t, eliminating v_t from the right-hand side by $(5.47)_1$, and solving the resulting differential equation for η_t numerically. This is equivalent to replacing $(5.47)_1$ by

$$\begin{aligned}
\chi_\xi &= -\frac{3(1-\xi)}{2u}\,[w(w v_\xi)_\xi + v], \qquad \chi(0,t) = 0,\\
u_t &= \frac{\chi}{1-\xi}\,u_\xi + w(w v_\xi)_\xi + v,
\end{aligned} \tag{5.48}$$

where χ replaces $v\eta_t$. The convective term u_ξ in $(5.48)_2$ was discretized using second-order upwinding that depends on the sign of χ; for details see, e.g., Kopteva (1996).

In our computations, we used the initial condition

$$v \propto \exp\left\{-\frac{a\eta^2}{\eta+1}\right\} \quad \text{at} \quad t = 0, \tag{5.49}$$

since it follows from (5.26) that if $v_0'(s = \frac{1}{2}) = -a$, then $v \sim \exp(-a\eta)$ as $\eta \to \infty$. Figure 6 shows snapshots of the relaxation of the solution towards the steady state, while Figure 7 shows the margin evolution. We have checked the initial evolution of the margin against the asymptotic formula (5.45) and found excellent agreement. The results support the conjecture that the steady state solution is globally stable.

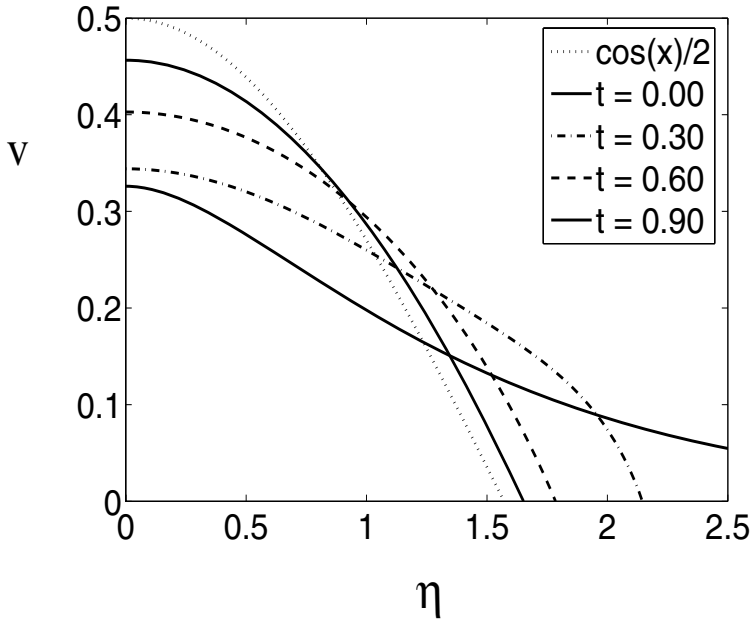

FIG. 6. *Relaxation of the solution of* (5.19) *to the steady state. The initial condition* $v_0(\eta)$ *(using the formulation in* (5.25)–(5.27)*) is given by* $v_0 \propto \exp\left\{-\frac{\eta^2}{\eta+1}\right\}$.

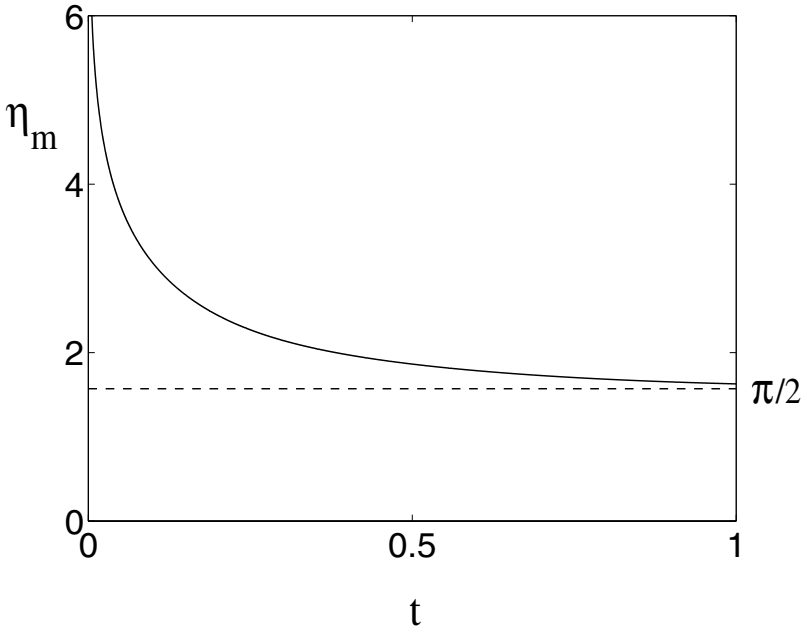

FIG. 7. *Evolution of the front position* η_m *as a function of* t *for the solution in Figure* 6. *The singularity at* $t = 0$ *is approximately (numerically) logarithmic.*

6. Conclusions. Beginning with a physics-based model of hillslope evolution and hydraulic drainage, we have shown how one can obtain a rational model for the local evolution of a stream or drainage channel. This model takes the form of a nonlinear diffusion equation with a nonlinear source term, similar to equations which have been much studied by analysts, but with the novelty of an additional integral constraint. The evidence we have gathered appears to indicate that this model is well-posed, and that its solution evolves to a unique steady state, with a width which is self-determining. This observation is interesting in view of the continuing difficulty in finding models of stream flow which can describe the stream width (see, for example, Parker (1978)).

A question of concern (but which is not addressed here) is that of putting our channel model within the context of the large scale evolution of hillslope topography. The way this can be done is as follows. As a river channel evolves, sediment is transported from the adjoining hillslope which is thus lowered. In a maturing hillslope, the channel thus eats its way down into the valley. In terms of the mathematical model, the channel will act as a thin, "shock-like" transition region between regions of hillslope with different gradients; it is a boundary layer connecting the different parts of the outer hillslope solution. Thus the results of the present paper can be used to provide a parameterization of the local channel dynamics in terms of the fluxes of sediment and water delivered from the surrounding hillslope, which evolves essentially via the Smith–Bretherton model. In this description, the hillslope evolves smoothly until it becomes concave, at which point a new channel will form. Specifically, this occurs where the characteristics of the water flow equation intersect, and the evolution of the head of the channel up the hillslope is determined by the point of shock formation. This is similar in tone but not in application to the discussion by Birnir, Smith, and Merchant (2001).

There are a number of interesting mathematical questions which deserve further study: the nonstandard eigenvalue problem (5.10) and (5.11), and the selection of front advance rate between (5.22) and (5.24), are two obvious ones. Of most concern in the application of the model to river system development is the fact that these channels grow (see (4.14)) when $S' > 0$; i.e., the hillslope is convex (upwards, in the sense of Figure 3). This is precisely the Smith–Bretherton condition which ensures that a uniform overland flow is stable. We thus have the paradoxical result that finite amplitude channels exist and are stable when the uniform steady state is also stable.

This observation is suggestive of bistability. We have not yet performed a study of the "rill" scaled model (4.2), but it is reasonable to expect it to have finite amplitude steady solutions, and these might plausibly connect to the uniform state branch at the linear stability, and "become" the channel branch as S' increases. It has to be said that it is not at all obvious how such a bifurcation diagram should be constructed. As with the other problems described above, this problem also awaits study.

Two other practical considerations deserve mention on this point. One is that our model assumes an unlimited sediment supply. In mature landscapes, erosion may become detachment limited (Howard 1994), and the form of the channel equation is somewhat changed. In essence, it appears that a similar equation may be appropriate in that case also but with a source term $H^{3/2}S^{3/2}$ which is independent of hillslope curvature.

The other comment is that in mature landscapes, such as that of Figure 1, it is evident that there will be flux of water and sediment to the channel; the hillslope is essentially three-dimensional, and it is possible that in such an altered geometry, the

conditions for channel formation are simply slope (and not curvature) dependent.

Acknowledgment. We thank Bruce Malamud for assistance with computer graphics.

REFERENCES

B. Birnir, T. R. Smith, and G. E. Merchant (2001), *The scaling of fluvial landscapes*, Comput. Geosci., 27, pp. 1189–1216.

G. F. Carrier, M. Krook, and C. E. Pearson (1966), *Functions of a Complex Variable*, McGraw–Hill, New York.

A. D. Howard (1994), *A detachment-limited model of drainage basin evolution*, Water Resour. Res., 30, pp. 2261–2285.

N. Izumi and G. Parker (1995), *Inception and channelization and drainage basin formation: Upstream-driven theory*, J. Fluid Mech., 283, pp. 341–363.

N. Izumi and G. Parker (2000), *Linear stability analysis of channel inception: Downstream-driven theory*, J. Fluid Mech., 419, pp. 239–262.

N. V. Kopteva (1996), *On the convergence, uniform with respect to a small parameter, of a four-point scheme for a one-dimensional stationary convection-diffusion equation*, Differ. Uravn., 32, pp. 951–957 (in Russian); Differential Equations, 32 (1997), pp. 958–964 (in English).

S. Kramer and M. Marder (1992), *Evolution of river networks*, Phys. Rev. Lett., 68, pp. 205–208.

D. S. Loewenherz (1991), *Stability and the initiation of channelized surface drainage: A reassessment of the short wavelength limit*, J. Geophys. Res., 96, pp. 8453–8464.

D. S. Loewenherz-Lawrence (1994), *Hydrodynamic description for advective sediment transport processes and rill initiation*, Water Resour. Res., 30, pp. 3203–3212.

E. Meyer-Peter and R. Müller (1948), *Formulas for bed-load transport*, in Proceedings of the International Association for Hydraulic Structures Research, 3rd Annual Conference, Stockholm, Sweden, pp. 39–64.

G. Parker (1978), *Self-formed straight rivers with equilibrium banks and mobile bed. Part* 1. *The sand-silt river*, J. Fluid Mech., 89, pp. 109–125.

A. A. Samarskii, V. A. Galaktionov, S. P. Kurdyumov, and A. P. Mikhailov (1995), *Blow-Up in Quasilinear Parabolic Equations*, de Gruyter Exp. Math. 19, de Gruyter, Berlin.

R. Slingerland, J. W. Harbaugh, and K. P. Furlong (1994), *Simulating Clastic Sedimentary Basins: Physical Fundamentals and Computer Programs for Creating Dynamic Systems*, Prentice–Hall, Englewood Cliffs, NJ.

T. R. Smith and F. P. Bretherton (1972), *Stability and the conservation of mass in drainage basin evolution*, Water Resour. Res., 8, pp. 1506–1529.

T. R. Smith, B. Birnir, and G. E. Merchant (1997a), *Towards an elementary theory of drainage basin evolution:* I. *The theoretical basis*, Comput. Geosci., 23, pp. 811–822.

T. R. Smith, B. Birnir, and G. E. Merchant (1997b), *Towards an elementary theory of drainage basin evolution:* II. *A computational evaluation*, Comput. Geosci., 23, pp. 823–849.

T. R. Smith, G. E. Merchant, and B. Birnir (2000), *Transient attractors: Towards a theory of the graded stream for alluvial and bedrock channels*, Comput. Geosci., 26, pp. 541–580.

K. Stewartson and J. T. Stuart (1971), *A non-linear instability theory for a wave system in plane Poiseuille flow*, J. Fluid Mech., 48, pp. 529–545.

G. E. Tucker and R. L. Slingerland (1994), *Erosional dynamics, flexural isostasy, and long-lived escarpments: A numerical modeling study*, J. Geophys. Res., 99, pp. 12229–12243.

E. W. Welsh, B. Birnir, and A. L. Bertozzi (2006), *Shocks in the evolution of an eroding channel*, Appl. Math. Res. Express, 71638.

G. Willgoose, R. L. Bras, and I. Rodríguez-Iturbe (1991), *A coupled channel network growth and hillslope evolution model:* I. *Theory*, Water Resour. Res., 27, pp. 1671–1684.